Egyptian Journal of Chemistry

http://ejchem.journals.ekb.eg/

In-Situ Fabrication of Polyurethane Acrylate/Zinc Oxide NPs Frameworks as dual-function Water-borne Binders for Blend Fabrics Printing

Fatma El Shall [1]* and Mona Al-Shemy [2]

[1] *National Research Centre, Dyeing, Printing and Textile Auxiliary Department, 33El-Bohouth St. (Former El-Tahrir St.), Dokki, P.O. 12622, Giza, Egypt.* [2] *National Research Centre, Cellulose and Paper Department, 33El-Bohouth St. (Former El-Tahrir St.), Dokki, P.O. 12622, Giza, Egypt.*

Abstract

In this work, compounds that may be utilized as multifunctional binding materials were developed with the goal of enhancing both the functional and color qualities of the printed apparel without requiring the application of extra pre-treatments or finishing techniques. Accordingly, two water-borne polyurethane acrylates (PUA), with an aliphatic and an aromatic isocyanate base, were utilized for the in-situ synthesis of zinc oxide (ZnO) nanoparticles via a facile and green route. Next, the fabricated PUA/ZnO nanocomposite frameworks were employed as dual-function binders in the pigment printing of blend fabrics (cotton/polyester and wool/polyester). By using UV-visible, FTIR and TEM tools, it was possible to verify that the produced nanocomposites had successfully formed polymer/metal oxide NP frameworks. The fabricated PUA/ZnO nanocomposite suspensions and printed blend fabrics demonstrated considerable antimicrobial activity against gram-positive and gram-negative bacteria. Additionally, the color strength and fastness properties of printed blend fabrics using the prepared binders were improved, particularly for cotton/polyester blends. Also, a significant enhancement in ultraviolet protection activity within nanocomposite-printed textiles was observed.

Keywords: Textile binder; Polyurethane acrylate; Zinc Oxide (ZnO) NPs; Pigment printing; Blend fabrics; UV blocking; Antimicrobial activity.

1. Introduction

Polyurethanes (PUs) are major thermoset and thermoplastic polymeric material family. Different polyol and polyisocyanate formulations can be employed to control and adjust their behavior. The urethane bond (HN-COO) can be generated through the interaction of one reactant's isocyanate group with the alcohol group of different components. Polymers with a significant number of urethane linkages are referred to as PUs, regardless of their molecular structure [1–5]. They are utilized in a wide range of industries, including the furniture and insulation industries, where flexible and rigid foam are used. In addition to their application in sealants, elastomers, and coatings, thermoplastic PUs are also commonly utilized in footwear and medical devices [4, 6, 7].

Since they minimize volatile organic emissions, water-borne polymer emulsions such as polyurethane aqueous dispersions are an important class of polymer materials, particularly in coating and paint applications. They are expected to perform basically as well as conventional solvent-borne systems [6]. Growing interest in and quick development of green and clean UV-curable polyurethane acrylate oligomers have occurred in light of acrylic's outstanding outdoor durability in addition to its fast curing rate and polyurethane's adaptable features such as impact strength, abrasion resistance, flexibility (at

*Corresponding author e-mail: fn.taha@nrc.sci.eg.
Received 22 May 2023, Revise Date: 20 June 2023; Accept Date 25 June 2023
DOI: 10.21608/EJCHEM.2023.212517.8003

low temperatures), controllable transparency, and hardness. However, there are only a few reports on the preparation and use of multifunctional, eco-friendly polyurethane binders for textile finishing applications [8, 9].

In recent times, the use of hybrid materials in the form of nanostructures that combine the advantages of organic and inorganic materials has received a lot of attention [10]. By incorporating nano-sized inorganic particles into an organic matrix, nanocomposites with exceptional mechanical and electrical properties can be developed [11]. Impregnating functional additives into PUs, such as CNT, clay, metal oxides (ZnO, TiO_2, CuO, and CeO_2), graphene, and hydroxyapatite, is the most commonly used method for improving the mechanical properties and thermal stability of PUs and expanding their potential applications [12–14].

Zinc oxide is a non-toxic, antibacterial, UV-shielding metal with antimicrobial and outstanding optical characteristics. The three main benefits of ZnO are its non-toxicity, lack of harmful effects on human cells, and low cost [12, 13, 15, 16]. These properties have led to its widespread use in polymer composites, antimicrobials, cosmetics, and optical devices [17]. Recently, environmentally friendly preparation of metal or metal oxide nanoparticles using a green approach has gained a lot of interest. Many adverse effects from chemical and physical processes can be avoided by using algae, plants, bacteria, actinomycetes, and fungi in the green synthesis of NPs, which results in the NPs being generated spontaneously under safe conditions of pH, temperature, and pressure without the need for hazardous or toxic ingredients or the addition of external capping, reducing, or stabilizing agents [16, 18, 19].

One of the growing human health issues is the UV protection of textiles. UV exposure can result in early skin ageing, and sun damage symptoms include liver spots, leathery skin, solar elastosis, and wrinkles. Moreover, exposure to UV radiation can result in corneal burns or inflammation, both of which can impair eyesight [15]. Due to its high excited binding energy (60 meV) and wide bandgap energy (3.37 eV), ZnO exhibits exceptional blocking activity against harmful UV rays [20].

The present work was carried out with the following objectives: in-situ synthesis of polyurethane acrylate oligomers (based on both aliphatic and aromatic isocyanate routes) and zinc oxide NPs frameworks, and their utilization as multifunction aqueous binders (binding agents with antimicrobial behavior and ultraviolet blocking activity) for printed cotton/polyester and wool/polyester blend fabrics using pigment color.

2. Experimental

2.1. Chemicals

Polypropylene glycol (PPG) (2000g/mol) was supplied by Fluka Chemical [Co. Switzerland)], Germany. Hydroxyl propyl methacrylate (HPMA) was supplied by Degussa, Germany. N, N-dimethylformamide (DMF) from ACROS Chemical Co. All chemicals were oven dried before being used. Dibutyltin dilaurate (DBTDL), isophorone diisocyanate (IPDI), toluene diisocyanate (TDI), and sorbitol were supplied by across Chemical Co, used as received. Zinc acetate LR was supplied by S.D.Fine-Chem LTD. Ammonium persulfate, as thermal initiator, was purchased from Merck-Germany. Bercolin CPK was supplied by Berssa-Turkey, as thickening agents. Bercolin metal CM as commercial binder was supplied by Berssa, Turkey. Cotton/polyester blend (CO/PET) fabric (50/50 %, 135 g/m^2) was provided by Misr Company for Spinning and Weaving, Mehalla El – Kubra, Egypt. Wool/polyester (W/PET) fabric (50/50) of 146 g/m^2 purchased from Goldentex Company. M.D yellow 2G pigment was supplied by Daico for the chemical industry, Cairo, Egypt. All chemicals utilized in this work are of analytical grade and used as received without further purifications.

2.2. Synthesis of Polyurethane Acrylate/Zinc Oxide NPs Framework

According to the modified approach previously reported [21], the reaction of polypropylene glycol with isophorone diisocyanate was carried out as follows:

Under a nitrogen atmosphere and a heated oil bath, a specified amount of polypropylene glycol (PPG) (2000 g/mol) and sorbitol were added in DMF (solvent) into a three-necked flask fitted with a stirrer, thermometer, and reflux condenser. To ensure that the reaction mixture was thoroughly mixed, the reactant was left at 40 °C for about an hour. Over a period of more than an hour, a calculated amount of IPDI and/or TDI containing 0.05 (w/w) DBTDL as catalyst was gradually added to the reaction mixture at 40°C in the case of IPDI and 30 °C in the case of TDI.

To achieve a satisfactory reaction rate without gelation, the mixture was agitated for an additional two hours at 60 °C. The mixture was allowed to react until the theoretical NCO content was achieved (the

end point at this stage was detected using a standard dibutylamine back-titration method) [22].

Once more, the reaction temperature was decreased to 45–50 °C. Over the course of an hour, a calculated amount of hydroxypropyl methacrylate (HPMA) was gradually added to the reaction mixture. The reaction was allowed to continue with no further temperature change for two hours of vigorous stirring after the addition of the HPMA. To prevent the potential for excessive heat crosslinking on unsaturated system sites, a lower reaction temperature was recommended. During this phase of the reaction, there was a noticeable shift in the viscosity of the reaction mixture. The PUA formed was a viscous, clear liquid; simply adding HPMA reduced its viscosity dramatically. After a few minutes of addition, the viscosity of the reactants begins to rise once more. As a result, at the end of the reaction, a thick, viscous liquid was formed.

In 50 mL of distilled water, 10 mL of the generated PUA is neutralized. Under vigorous stirring, the neutralized solution's temperature was raised to 50 °C for 30 minutes. The resulting solution was subsequently filtered. The filter solution was then added to 10 mL of 0.1 mol zinc acetate dihydrate, Zn $(CH_3COO)_2.2H_2O$, and stirred for an hour at 70–80 °C under alkaline conditions (pH 11) that were gradually adjusted by adding 0.1 mol NaOH. The emulsions were miniemulsified via ultrasonication in an ice bath for 6 minutes. To avoid any potential photoreaction, PUA and ZnO dispersions have been stored in a black bottle.

2.3. Printing of Textile Fabric

In fabric printing, the pigment paste formula contains 50 g/L pigment, 100 g/L binder (commercial) or 10 g/L for papered PUA/ZnO, 40 g/L thickener, 10 g/L ammonium persulfate, and Y distilled water. The printing paste was prepared according to the earlier formula, homogenized, and then applied to the fabric surfaces using the flat silk-screen printing process. The printed textiles were thermally fixed in an automated thermal oven (Wemer Mathis Co., Switzerland) at 160°C for 5 minutes. Following fixation, the printed fabrics were washed with cold water, hot water, and cold water, successively, to remove excess thickener and unreacted materials.

2.4. Characterization

The materials' FTIR spectra were recorded using a JASCO FT-IR 6100 spectrometer (Tokyo, Japan). Transmission measurements were taken between 400 and 4000 cm^{-1}, with 60 scans and a resolution of 4 cm-1. The JASCO V-730 UV-visible/NIR double-beam spectrophotometer, Tokyo, Japan, was used to perform UV-Vis spectrophotometer measurements. Transmission electron micrographs of nanocomposite polymers were obtained using a high-resolution JEOL JEM-2100 Transmission Electron Microscope (Japan). Color strength (K/S) and color parameters L (representing darkness to lightness), a (representing greenness to redness), and b (representing blueness to yellowness) of printed fabrics were assessed using the Mini Scan TM XE Hunter-Lab Universal Software, which is based on the Kubelka Munk equation, K⁄S = (1 - R)2⁄2R, Where K denotes the absorption coefficient, S denotes the scattering coefficient, and R denotes the fraction of light reflected at a wavelength of minimum-maximum absorbance. The ultraviolet protection factor (UPF) was estimated using an AATCC Test Method 183:2010-UPF using a UV-Shimadzu 3101-PC-Spectrophotometer (UPF >50 indicates strong UV protection). Fastness to washing was measured according to launder-metre AATCC Test Method 61-2013. The fastness to light, rubbing, and perspiration measurements were done according to the standard methods of AATCC 1993a, 1993b, and 1993c, respectively. Electron Dispersion Emission X-ray (EDX): Elemental analysis of printed fabrics by both prepared binders was recorded by energy-dispersive X-ray spectroscopy (EDX) using a Quanta FEG-250 microscope at a voltage of 10 kV.

2.5. Antibacterial test

The fabricated PUA/ZnO nanocomposites suspensions and printed fabrics were quantified for antimicrobial activity against different microbial species: gram-positive bacteria [*Bacillus subtilis* (ATCC 6633) and *Staphylococcus aureus* (NRRLB-767)], gram-negative bacteria [*Escherichia coli* (ATCC 25922) and *Pseudomonas aeruginosa* (ATCC 10145)], yeast [*Candida albicans* (ATCC 10231)], and fungus [*Aspergillus niger* (NRRLA-326)]. Quantitative tests were performed using liquid media (LB Broth). All tubes (5 mL) of nutrient broth were inoculated with 50 µl of bacterial culture and assessed for antimicrobial activity by adding samples, then incubated in a shaking incubator at 37 °C for 24 h. Microbial growth was measured at 620 nm, and the results were expressed as a growth inhibition percentage [23]. All the results were expressed as averages of at least three tests.

3. Results and discussion

3.1. Synthesis and characterization of polyurethane acrylate zinc oxide (PUA/ZnO) NPs frameworks

Typically, polyether or polyester polyol, when reacting with isocyante compounds in the presence of a catalyst and chain extender, generates polyurethanes, which are subsequently further capped with an acrylate terminal hydroxyl compound. Under carefully controlled conditions and catalyst dose, one or two hydroxyl groups from PPG and/or sorbitol interact with the primary isocyanate group of isocyanate compounds to generate an isocyanate-terminated polyurethane pre-polymer, leaving the remaining isocyanate group unreacted for a subsequent reaction with HPMA to generate unsaturation sites on the polyurethane prepolymer ends to form polyurethane acrylate. Sorbitol, a bio-based compound, could be used as a chain extender to enhance the ability of cross-linking and hydrogen bond formation in acrylated urethanes. This eventually results in a pre-polymer with a higher molecular weight and better flexibility, which is subsequently capped by the HPMA monomer. Having the same functionality, polyurethane acrylates generated from aliphatic isocyanates (A), such as IPDI, are much more flexible pre-polymers than aromatic-based ones (R) [21, 22]. The key advantage of aliphatic polyurethane acrylate (A) is that it is basically non-yellowing and can therefore be employed to produce long-lasting coatings on white or light-colored materials. However, the aromatic base PUA(R) is less expensive and offers enhanced UV shielding properties, favoring its outdoor application [6, 21].

The function groups that characterize the formation of polyurethane acrylate as PUA(A) and PUA(R) were evidenced through FTIR spectra, as illustrated in Figure 1a and 1b, respectively, by the emergence of bands at around 843 and 830 cm^{-1} corresponding to ν: -C-H. Bands appeared at 955 and 940 cm^{-1} are for δ: =C-H. Also, strong absorption bands characteristic of st C-O-C were noticed at around 1104 and 1153 cm^{-1}. The bands at 1343 and 1344 cm^{-1} could be assigned to st-C-N. The δ: CH_2 band was located at 1466 and 1468 cm^{-1}. The bands at 1547, 1549 cm^{-1} corresponded to δ: N-H, while the bands at 1713 and 1733 cm^{-1} corresponded to st C=O [24]. st C=C located at 1935 and 1966 cm^{-1}, appeared as three bands in a conjugated double bond of an aromatic ring and as two bands in the case of an alicyclic ring. st-CH_2, CH_3, and CH are located at around 2882 and 2884 cm^{-1}. Bands at 3335 and 3470 cm^{-1} were attributed to st N-H and unbonded OH groups [17, 21, 25, 26].

It is clear from the spectra in Figure 1 that no absorption band was observed at approximately 2270 cm^{-1}, which corresponds to the N=C=O group. This indicates that the entire amount of either IPDI or TDI was consumed during the reaction, and the fact that the final product is free from isocyanates indicates the success of the addition polymerization process and the formation of polyurethane acrylate (PUA) [13, 27].

The in-situ fabrication of ZnO NPs in aqueous dispersion of waterborne polyurethane acrylate was done through hydroxyl and urethane groups, which were utilized as reducing and stabilizing agents for ZnO NPs. The polymeric material may be physically adsorbed into the layer of ZnO through solution, where it also serves as a steric stabilizer as well as helping hydrophobize ZnO particles. Moreover, the acrylate moiety in the PUA within the ZnO surface could participate in the photo-polymerization of PUA and form covalent links with the polymer matrix [17].

FTIR spectroscopy was also employed to monitor the successful fabrication of PUA/ZnO NPs composites both PUA (A) and (R)/ZnO (Figure 1). When compared with the neat PUA spectrum, peaks in the spectra of both PUA (A) and (R)/ZnO showed noticeable shifts and changes as a result of the interaction between PUAs and ZnO particles [28]. It is evident from the spectra that -OH has formed on the surface of ZnO through the formation of a broad band in the ranges from 3644 to 3023 cm^{-1} and 3631 to 3071 cm^{-1} of PUA(A)/ZnO and PUA(R)/ZnO, respectively [28]. The presence of spectra peaks at 490, and 792 cm^{-1} in the PUA(A)/ZnO and 470, and 798 cm^{-1} in the PUA(R)/ZnO confirmed the formation of the νZn-O moiety in far infrared region [13, 16, 28]. Additionally, there is a considerable –NH- deformation vibration of fabricated ZnO nanocomposites at 1544 cm^{-1} for PUA (A)/ZnO and 1540 cm^{-1} for PUA (R)/ZnO [28]. As a result, the FTIR spectra clearly demonstrates the successful incorporation of ZnO NPs in the fabricated composites [10, 29].

Ultraviolet (UV) spectroscopy is one of the most commonly used approaches for evaluating the structural properties of metal nanoparticles. The spectra of these nanoparticles exhibit strong absorption bands in contrast to the bulk metal or metal oxide [30]. PUA/ZnO NPs' UV-visible spectra were recorded between the wavelengths of 200 and 800 nm. The UV-visible absorption spectra of PUA(A)/ZnO and PUA(R)/ZnO NPs are displayed in Figure 2. With maximum peaks at 260 and 376 nm characteristic of the surface plasmon resonance of ZnO NPs, this is another clue to the successful formation of nanocomposites. The difference in the maxima wavelength between the two PUA (A)/ZnO and PUA (R)/ZnO could be related to their different

particle size distribution [31]. Zinc oxide exhibits a dramatic increase in absorbance below 380 nm. With decreasing particle size, there is both a decrease in absorbance and a blue shift in the curves to lower wavelengths because of the excitations' quantum confinement [32–34].

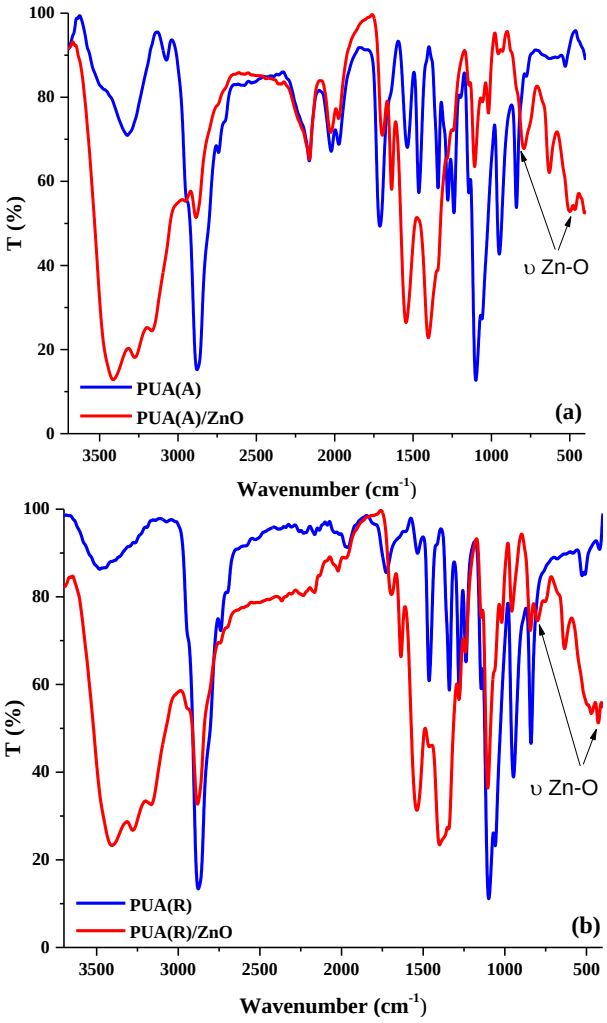

Figure 1. FTIR spectra of (a) PUA(A), PUA(A)/ZnO, and (b) PUA(R), PUA(R)/ZnO nanocomposite.

Figure 3 displays TEM images of PUA(A)/ZnO and PUA(R)/ZnO NPs. The images demonstrate that the particles' sizes ranged from 20 to 38nm. The high surface energy of ZnO NPs, which causes aggregation under the influence of the aqueous fabrication medium, may be the explanation of the aggregation and narrow size dispersion distribution of PUA(A)/ZnO (Figure 3a) [35, 36]. On the other hand, PUA(R)/ZnO nanocomposite is typically spherical (Figure 3b). As a result, compared to PUA(A)/ZnO from TEM images, the PUA(R)/ZnO nanocomposite is more isolated and homogeneous. It was reported that the degree of compatibility between the polymer layer that's adsorbed on the ZnO particle surface and the specific polymer matrix would be a major factor in an inorganic nanoparticle's ability to disperse in a polymer matrix [17].

ZnO NPs are now classified as broad-spectrum antibacterial agents. As a result, ZnO NP applications have expanded beyond traditional boundaries into new areas of interest like fabrics, medicine, and cosmetics. Thus, while PUA(A)/ZnO exerts antimicrobial effectiveness against *Bacillus subtilis* and *Pseudomonas aeruginosa*, PUA(R)/ZnO acts as an active antimicrobial agent against *Bacillus subtilis*, *Staphylococcus aureus*, *Escherichia coli*, *Pseudomonas aeruginosa*, and *Aspergillus niger*. In light of this, the suspensions of nanocomposites created for this investigation revealed divergent bactericide efficacy among the tested microbes (Table 1). Each PUA/ZnO nanocomposite's antibacterial activity in the test varied in its effectiveness due to variations in the electrostatic interaction between the functional groups of PUA (A and R) and ZnO NPs, which is dependent on the structure, charge, and chemical composition of the polymer.

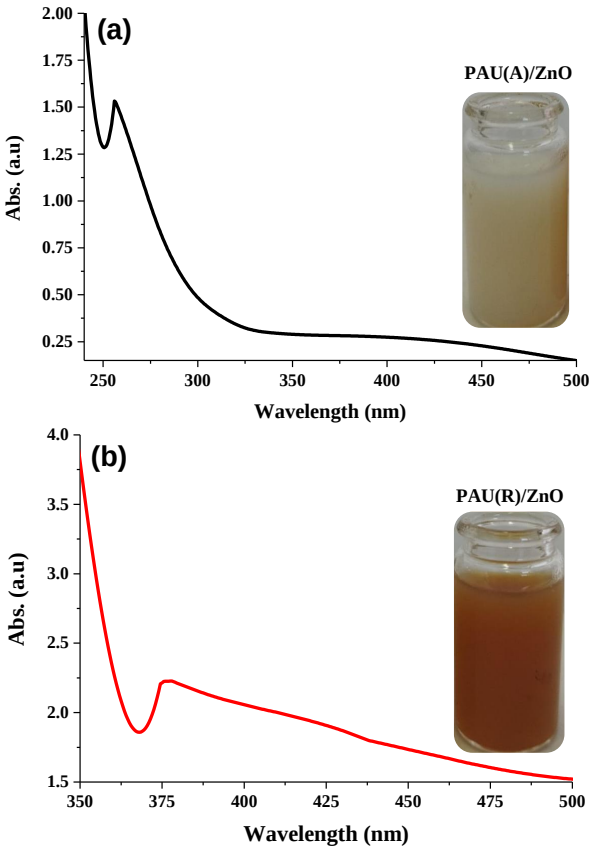

Figure 2. UV-visible spectra and photographic image of (a) PUA(A)/ZnO NPs and (b) PUA(R)/ZnO NPs.

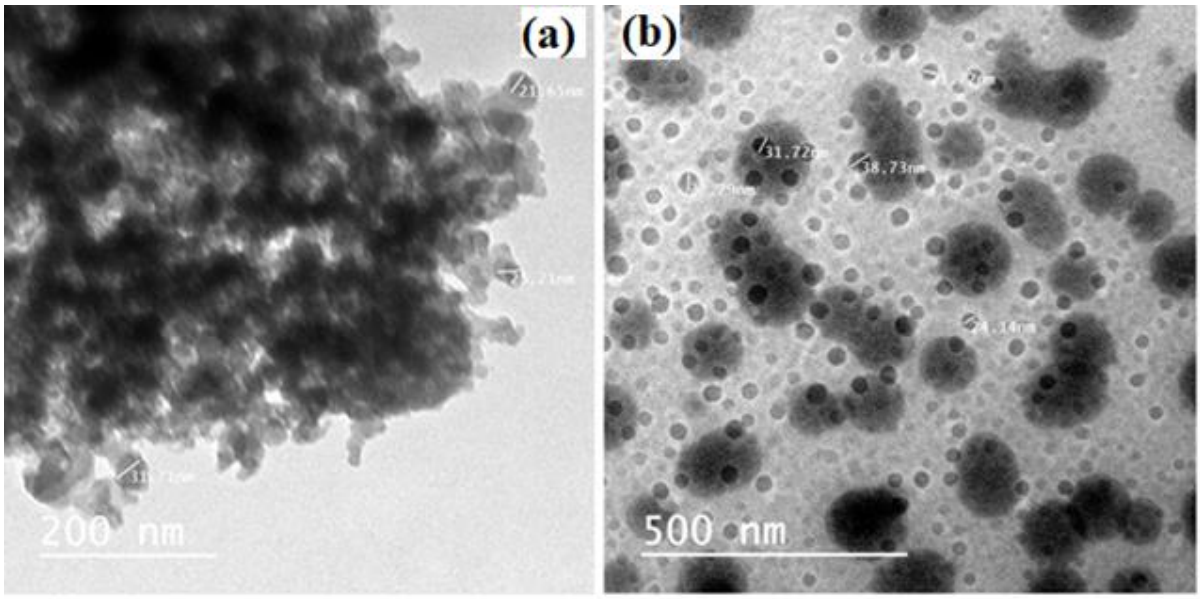

Figure 3. TEM images of (a) PUA(A)/ZnO NPs and (b) PUA(R)/ZnO NPs.

Table 1. Antibacterial activity of PUA/ZnO nanocomposites suspensions.

Sample	*Bacillus Subtilis*	*Staphylococcus aureus*	*Escherichia coli*	*Pseudomonas aeruginosa*	*Candida albicans*	*Aspergillus Niger*
PUA(A)/ZnO	27.04 ± 0.74	- ve	-ve	51.24 ± 0.62	- ve	- ve
PUA(R)/ZnO	26.87 ± 0.54	44.72 ± 0.71	32.65 ± 0.	67.19 ± 0.59	- ve	50.77 ± 0.44
Ciprofloxacin	96.01 ± 0.24	97.24 ± 0.31	98.07 ± 0.28	98.10 ± 0.25	-ve	-ve
Nystatin	-ve	-ve	-ve	-ve	97.16 ± 0.34	98.23 ± 0.37

3.2. Application of papered composites as binders in pigment printing of polyester/cotton and polyester/wool blend textile fabrics

Pigment fixation on textiles requires a binding agent that, under fixing or curing conditions, develops into a continuous film that traps the colorant particles inside. In this regard, polymers or, more preferably, copolymers of unsaturated monomers such as acrylonitrile, butadiene, styrene, ethyl acrylate, and vinyl acetate can serve well as binding agents. Since the properties of the binding agent are related to all of the fastening behaviors of printed garments, the overall properties of the binding agents should be improved to improve the overall performance of the textile-pigmented products [21, 37]. The curing process can be carried out appropriately, depending on the available curing source and the material that needs to be treated. Considering that the generated binder contains several functional groups that respond differently through the curing process, such as acrylate groups that can be radially cured by UV rays as well as hydroxyl groups that can be thermally cured, as a dual-curing waterborne binder, this is regarded as an excellent added value to the prepared PUA/ZnO composites [25, 38, 39].

To demonstrate the curing mechanism of a water-based dual-cure urethane-acrylate, the following steps might possibly occur: The dried ZNO/PUA particles were either cured in the presence of peroxide (thermal initiator) or by short-term UV irradiation under the influence of a photo-initiator. Following a short period of heating, water was released. Heat promotes the thermal breakdown of peroxide, resulting in free radicals capable of initiating both polymerization and oxidation of the double bonds of terminal acrylate groups. As a result, the acrylate double bonds are broken, forming a cross-linked layer that fixes the pigment inside Figure 4 [25].

The color depth (K/S) and color parameter values of cotton/polyester (CO/PET) and wool/polyester (W/PET) fabrics with pigment printing are shown in Table 2 using commercial binder at a standard concentration of 100 g/L and synthesized PUA/ZnO NPs nanocomposites at a concentration of 10 g/L. In accordance with the results, all printed textiles using printing paste, including synthesized aromatic and

aliphatic bases and polyurethane/ZnO composites, appeared to have improved color depth when compared to fabrics printed using commercial binder. The ability of urethane groups to develop intermolecular hydrogen bonds improved the binding strength of PUA/ZnO. Moreover, the ether, urea, and urethane groups (electronegative elements) interacted with the ZnO's surface hydroxyl group to create a strong binding that increased the adhesive power and crosslinking density of the formed film [12, 40].

According to the data obtained from evaluating color parameters, i.e., from L, unlike samples printed with the commercial binder, almost all printed fabrics with PUA/ZnO nanocomposites exhibited a darker color shift (higher color depth). However, even PUA/ZnO nanocomposites exhibited a darker color shift (higher color depth). However, even though all printed samples exhibited a yellow shift, samples with PUA/ZnO, except for the W/PET$_{PUA(R)/ZnO}$, displayed the ideal yellow shift.

Table 2 also highlighted the UPF ratings of printed fabrics. Many prior investigations stated that specific metal oxide NPs might scatter UV light at wavelengths between 200 and 400 nm due to their small size (between 20 and 40 nm) and large surface area. Further, NPs reach their UV scattering maximum when NP sizes a tenth of the scattering wavelength [41, 42]. Both printed CO/PETC and W/PETC fabrics demonstrated high UV blocking activity, which may be related to the fabric structure

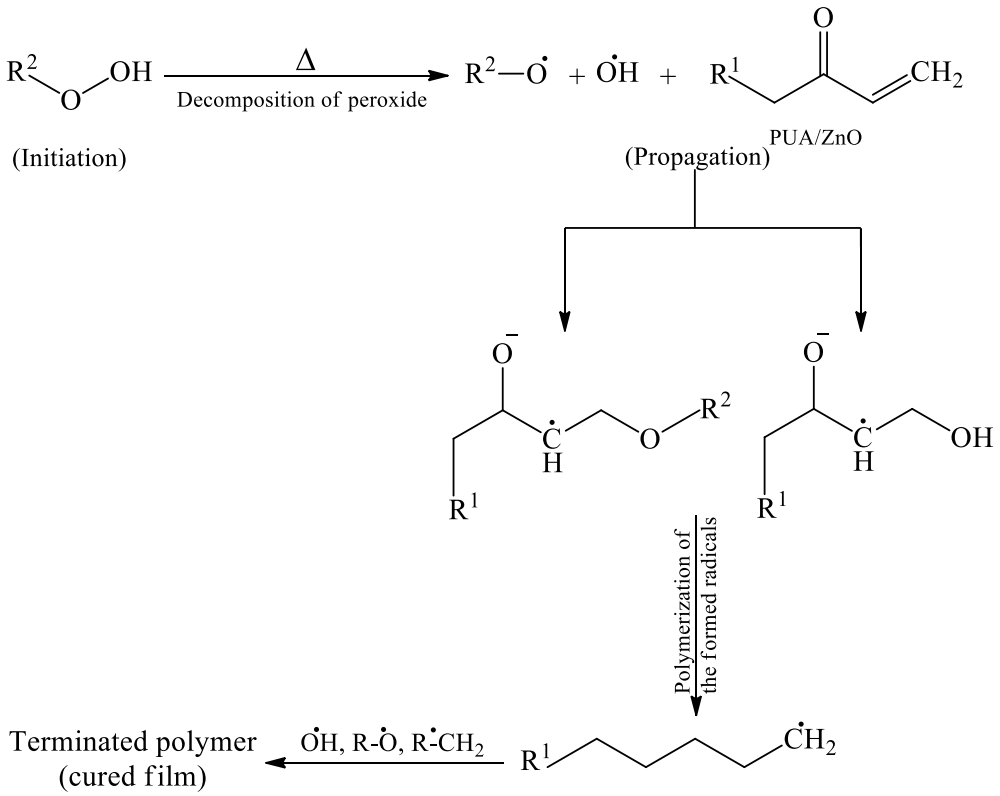

Figure 4. Thermal curing mechanism of PUA/ZnO.

According to the data obtained from evaluating color parameters, i.e., from L, unlike samples printed with the commercial binder, almost all printed fabrics with independent of the coating material. This may be due to the polyester element's aromatic units' better UV absorptivity [11, 35, 36].

Table 2. K/S, color parameters, and UPF values of printed fabrics.

Sample	K/S λ=480nm	L	a	b	UPF
CO/PET$_C$	0.77	68.74	10.92	10.12	98.0
CO/PET$_{PUA(A)/ZnO}$	1.00	64.42	10.30	8.84	196.5
CO/PET$_{PUA(R)/ZnO}$	1.14	63.72	14.59	9.67	298.4
W/PET$_C$	1.06	62.44	7.94	7.52	45.7
W/PET$_{PUA(A)/ZnO}$	1.23	60.19	7.48	7.37	154.1
W/PET$_{PUA(R)/ZnO}$	1.10	65.08	11.87	10.17	192.9

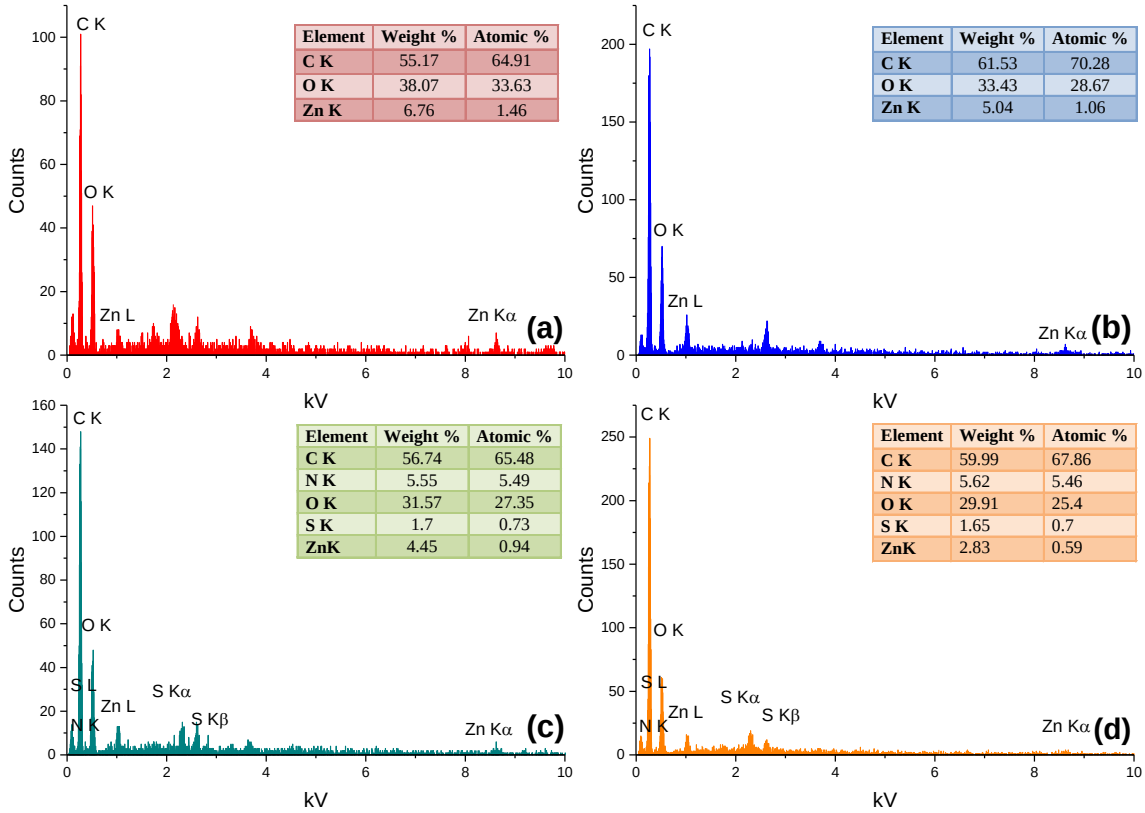

Figure 5. EDX graphs of CO/PET$_{PUA(A)/ZnO}$ (a), CO/PET$_{PUA(R)/ZnO}$ (b), W/PET$_{PUA(A)/ZnO}$ (c), and W/PET$_{PUA(R)/ZnO}$ (d) printed fabrics.

The results revealed that utilizing of synthesized PUA/ZnO as binding agents in pigment printing of blend fabrics have a significant positive influence on the ability of printed fabrics to shield UV rays, potentially reducing the detrimental effects of daylight UV rays on the human body. This may due to the dual effect of both ZnO NPs and C=C double bonds of PUA acrylate part of PUA/ZnO [35, 36, 43–45].

In general, the blocking activity of printed fabrics was significantly improved by appling synthesized PUA/ZnO as binders. the higher reactivity of aromatic ring related to the delocalization of electron pair over aromatic ring structure in PUA(R)/ZnO, which may also provide extra blocking activity side by side with ZnO, may be the reason why higher enhancement in blocking activity was observed with the PUA(R)/ZnO printed samples compared with PUA(A)/ZnO prints [43, 45, 46].

When compared to CO/PET$_c$, the UV blocking activity of printed CO/PET$_{PUA(A)/ZnO}$ and CO/PET$_{PUA(R)/ZnO}$ textiles was significantly enhanced. As previously demonstrated, greater enhancement was observed with the CO/PET$_{PUA(R)/ZnO}$ printed sample. Additionally, PUA(A)/ZnO and PUA(R)/ZnO printed W/PET fabrics showed

Table 3. Fastness properties of printed fabrics.

Fabric	Rubbing		Washing fastness		Perspiration			
					Acidic		Alkaline	
	Dry	Wet	St.[1]	Alt.[2]	St.[1]	Alt.[2]	St.[1]	Alt.[2]
CO/PET$_C$	2-3	2-3	3	4	4-5	4-5	4-5	4-5
CO/PET$_{PUA(A)/ZnO}$	3-4	3	3-4	4	4-5	4-5	4-5	4-5
CO/PET$_{PUA(R)/ZnO}$	3-4	3	4	4	4-5	4-5	4-5	4-5
W/PET$_C$	2-3	2-3	3	4	4-5	4-5	4-5	4-5
W/PET$_{PUA(A)/ZnO}$	3	3	3-4	4	4-5	4-5	4-5	4-5
W/PET$_{PUA(R)/ZnO}$	3	3	3-4	4	4-5	4-5	4-5	4-5

St.[1]=Staining; Alt.[2]=Alteration.

Table 4. Antibacterial activity of printed fabrics.

Fabric	Antimicrobial activity (%)			
	Bacillus subtilis	***Staphylococcus aureus***	***Escherichia coli***	***Pseudomonas aeruginosa***
CO/PET$_C$	0	0	0	0
CO/PET$_{PUA(A)/ZnO}$	29.09±0.21	0	23.94±0.69	28.69±0.11
CO/PET$_{PUA(R)/ZnO}$	24.69±0.81	0	18.61±0.74	71.75±0.55
W/PET$_C$	0	0	0	0
W/PET$_{PUA(A)/ZnO}$	29.89±0.20	53.49±3.86	12.75±0.59	40.91±0.09
W/PET$_{PUA(R)/ZnO}$	0	0	33.58±0.78	48.23±0.20

noticeably improved UV shielding performance in a pattern similar to CO/PET fabric, although to a lesser extent.

The EXD analysis of printed fabrics by prepared binder nanocomposites is shown in Figure 5. ZnO NPs were found during the EDX screening of the fabrics printed with paste containing PUA/ZnO nanocomposites. Compared to the printed W/PET, the printed CO/PET fabrics displayed a higher percentage of ZnO NPs. Moreover, the fabric printed with PUA(A)/ZnO seemed to have a higher ZnO percentage than the fabric printed with PUA(R)/ZnO.

According to the results in Table 3, the dry and wet rubbing fastness of all printed fabrics printed by PUA/ZnO binders exhibited some improvement when compared to printed fabrics produced by commercial binder. It is well established that a polymer or copolymer's ability to resist rub and how well it holds up during washing determines how effective it will be as a binding material and how well it will perform in printing processes estimating its quality. Consequently, this improvement in dry and wet rubbing fastness may be due to the prepared composite's ability to form a strong, regular, cohesive, and cross-linked film that resists the effect of friction and external scratch forces and reduces the release or exit of the color trapped inside.

Furthermore, printed fabrics performed well in terms of washing and perspiration fastness, and the binding power of both synthesized binders appeared to be comparable to that of commercial binders.

3.3. Antibacterial activity of printed fabrics

The viable cell colony count was used for the quantitative test on printed fabric (Table 4). The fabric printed with PUA(A)/ZnO and PUA(R)/ZnO

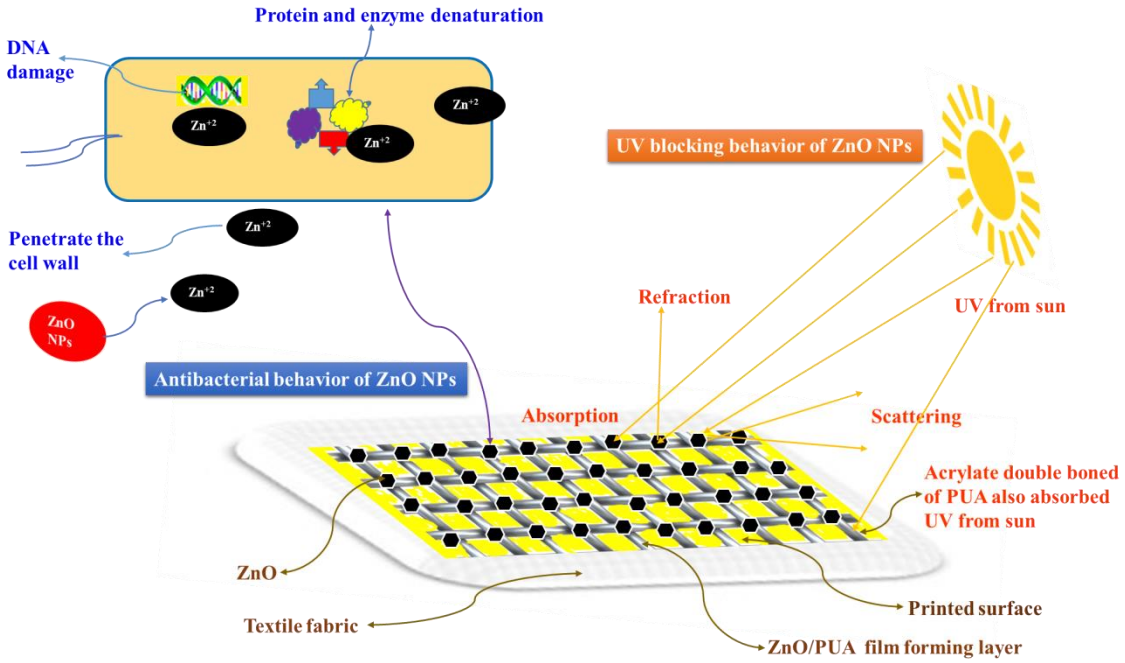

Figure 6. Schematic representation of how the blend fabric printed with prepared nanocomposite binders performed.

have displayed variable antibacterial activity against Gram-negative bacteria: *Escherichia coli* and *Pseudomonas aeruginosa* and Gram-positive bacteria *Bacillus subtilis* and *Staphylococcus aureus*. In comparison to CO/PET unprinted fabric, the CO/PET fabric printed with PUA(A)/ZnO and PUA(R)/ZnO exerted antibacterial behavior against *Bacillus subtilis*, *Escherichia coli*, and *Pseudomonas aeruginosa*. On the other hand, unlike the W/PET control fabric, the W/PET printed with PUA(A)/ZnO displays antibacterial efficiency against the four tested bacterial species, whereas those treated with PUA(R)/ZnO show antibacterial activity against only the gram-negative bacteria *Escherichia coli* and *Pseudomonas aeruginosa*. The results show that the efficacy of printed fabrics to prevent bacterial development differs depending on the microorganisms' species and fabric structure. ZnO NPs work against bacteria by releasing metal ions that enter the cell membranes and interfere with functional groups in proteins and nucleic acids. This prevents the enzymes from working as intended by preventing the metal ions' ability to penetrate the bacterial cell membranes. Thus, the modification of the cell structure will eventually result in the suppression of microbes [47, 48]. ZnO NPs may also exert their effects through the release of the active form of oxygen, which triggers electrostatic binding and changes DNA or enzyme pathways as well as the prokaryotic cell wall [49, 50]. Due to the mitochondrial, DNA, and membrane deterioration caused by this oxidative stress, bacteria die [51, 52]. In light of this, it is possible that the production of H_2O_2 on the surface of ZnO NPs, as suggested by numerous researchers, has the greatest effect on preventing bacterial growth. Finally, the performance of the fabricated nanocomposite binders can be schematically represented in Figure 6.

4. Conclusions

In this investigation, two water-borne polyurethane acrylates have been developed by the polyaddition reaction of polypropylene glycol, two isocyanate routes (isophorone diisocyanate and toluene diisocyanate), and the polymer chain extended by naturally occurring sorbitol, which is further caped by hydroxyl propyl methacrylate in the presence of DBTDL as catalyst. The prepared pre-polymers were utilized as reducing routes for facile fabrication of PUA/ZnO nanocomposites. FTIR scanning was employed to monitor the formation of PUA/ZnO nanocomposites. The approach highlighted the spectra changes that occurred throughout the development of both composites and displayed the distinctive peaks, which confirmed the successful fabrication of PUA/ZnO. The characteristic absorption peaks of ZnO NPs were recorded by a UV spectrophotometer. Spherical particles with nano-sized dimensions of PUA/ZnO nanocomposites were captured by TEM microscopy. Depending on the properties of the prepared nanocomposites and the nature of their functional groups, they were applied as multifunctional binding agents in printing blended fabrics with pigment colors. The two prepared PUA/ZnO were successfully used as binder, displaying improvements in color intensity and enhanced fastness properties. Additionally, printed fabrics have excellent potential to shield against the harmful impacts of ultraviolet light.

According to the antibacterial results of printed fabric, the fabric printed using the two PUA/ZnO nanocomposites had considerable antimicrobial behavior towards both Gram-positive and Gram-negative bacteria. This could be deemed an essential added benefit to the fabricated nanocomposite binders. In conclusion, these binders were developed to work as high-performance bonding agents that enhance the color properties of printed fabric while simultaneously providing printed goods with additional properties that increase the print's value and optimize its performance. In the current study, this was achieved in a single, straightforward process without requiring further treatments or finishing steps, providing a very high economic and environmental value.

5. Conflicts of interest

There are no conflicts to declare.

6. Funding sources

Financial support was received from National Research Centre, Egypt (Grant ID 13010304).

7. Acknowledgments

The authors appreciate the kind assistance of Dr. Muhammad Al-Awadi, Department of Microbial Biotechnology, National Research Centre, in conducting quantitative antimicrobial testing.

8. References

1. Zia KM, Bhatti HN, Ahmad Bhatti I (2007) Methods for polyurethane and polyurethane composites, recycling and recovery: A review. React Funct Polym 67:675–692. https://doi.org/10.1016/j.reactfunctpolym.2007.05.004
2. Blaj DA, Diaconu AD, Harabagiu V, Peptu C (2023) Polyethylene Glycol-Isophorone

Diisocyanate Polyurethane Prepolymers Tailored Using MALDI MS. Materials (Basel) 16:821. https://doi.org/10.3390/ma16020821

3. Engels HW, Pirkl HG, Albers R, et al (2013) Polyurethanes: Versatile materials and sustainable problem solvers for today's challenges. Angew Chemie - Int Ed 52:9422–9441. https://doi.org/10.1002/anie.201302766
4. De Souza FM, Kahol PK, Gupta RK (2021) Introduction to Polyurethane Chemistry. In: ACS Symposium Series. ACS Publications, pp 1–24
5. Mohamed M, Ramadan AM, Assem Y (2021) Soybean oil-based polyol as a modified natural binder for polyurethane turf-adhesive. Egypt J Chem 64:1093–1099
6. Sultan M, Zia KM, Bhatti HN, et al (2012) Modification of cellulosic fiber with polyurethane acrylate copolymers. Part I: Physicochemical properties. Carbohydr Polym 87:397–404. https://doi.org/10.1016/j.carbpol.2011.07.070
7. Qi G, Yang W, Puglia D, et al (2020) Hydrophobic, UV resistant and dielectric polyurethane-nanolignin composites with good reprocessability. Mater Des 196:109150. https://doi.org/10.1016/j.matdes.2020.109150
8. Karbalaei H, Tarmian A, Rasouli D, Pourmahdian S (2022) Effects of UV-curing epoxy acrylate and urethane acrylate coatings incorporated with ZnO nanoparticles on weathering resistance of thermally modified timber. Wood Mater Sci Eng 17:868–877. https://doi.org/10.1080/17480272.2021.1968491
9. Hu Y, Shang Q, Bo C, et al (2019) Synthesis and Properties of UV-Curable Polyfunctional Polyurethane Acrylate Resins from Cardanol. ACS Omega 4:12505–12511. https://doi.org/10.1021/acsomega.9b01174
10. Mishra RS, Mishra AK, Raju KVSN (2009) Synthesis and property study of UV-curable hyperbranched polyurethane acrylate/ZnO hybrid coatings. Eur Polym J 45:960–966. https://doi.org/10.1016/j.eurpolymj.2008.11.023
11. Kim D, Jeon K, Lee Y, et al (2012) Preparation and characterization of UV-cured polyurethane acrylate/ZnO nanocomposite films based on surface modified ZnO. Prog Org Coatings 74:435–442. https://doi.org/10.1016/j.porgcoat.2012.01.007
12. Rahman MM (2020) Polyurethane/zinc oxide (PU/ZnO) composite-synthesis, protective property and application. Polymers (Basel) 12:1535. https://doi.org/10.3390/polym12071535
13. Ariffin MM, Aung MM, Abdullah LC, Salleh MZ (2020) Assessment of corrosion protection and performance of bio-based polyurethane acrylate incorporated with nano zinc oxide coating. Polym Test 87:106526. https://doi.org/10.1016/j.polymertesting.2020.106526
14. Feng J, Fang L, Ye D (2018) Self-photoinitiated oligomers of water-diluted polyurethane acrylate grafted with zinc oxide of low concentrations. Prog Org Coatings 120:208–216. https://doi.org/10.1016/j.porgcoat.2018.04.004
15. Karthik S, Siva P, Balu KS, et al (2017) Acalypha indica–mediated green synthesis of ZnO nanostructures under differential thermal treatment: Effect on textile coating, hydrophobicity, UV resistance, and antibacterial activity. Adv Powder Technol 28:3184–3194. https://doi.org/10.1016/j.apt.2017.09.033
16. Dawwam GE, Al-Shemy MT, El-Demerdash AS (2022) Green synthesis of cellulose nanocrystal/ZnO bio-nanocomposites exerting antibacterial activity and downregulating virulence toxigenic genes of food-poisoning bacteria. Sci Rep 12:16848. https://doi.org/10.1038/s41598-022-21087-6
17. Zhang S, Zhang D, Bai H, Ming W (2020) ZnO Nanoparticles Coated with Amphiphilic Polyurethane for Transparent Polyurethane Nanocomposites with Enhanced Mechanical and UV-Shielding Performance. ACS Appl Nano Mater 3:59–67. https://doi.org/10.1021/acsanm.9b01540
18. Eissa D, Hegab RH, Abou-Shady A, Kotp YH (2022) Green synthesis of ZnO, MgO and SiO2 nanoparticles and its effect on irrigation water, soil properties, and Origanum majorana productivity. Sci Rep 12:. https://doi.org/10.1038/s41598-022-09423-2
19. Al-Shemy M, El-Shafie A, Alaneny A, Adel A (2023) Facile In-Situ Synthesis of Nanocrystalline Celluloses-Silver Bio-nanocomposite for Chitosan Based Active Packaging. Egypt J Chem 66:335–352. https://doi.org/10.21608/ejchem.2022.149568.6465
20. Vu Anh T, Pham TAT, Mac VH, Nguyen TH (2021) Facile Controlling of the Physical Properties of Zinc Oxide and Its Application to Enhanced Photocatalysis. J Anal Methods Chem 2021:1–12. https://doi.org/10.1155/2021/5533734
21. M. El-Molla M, Haggag K, N. El-Shall F, O. Shaker N (2012) Part 1: Synthesis and Evaluation of Novel Nano Scale Powdered Polyurethane Acrylate Binders. Adv Chem Eng Sci 02:212–227.

https://doi.org/10.4236/aces.2012.22026
22. Abdelrehim M, Komber H, Langenwalter J, et al (2004) Synthesis and characterization of hyperbranched poly (urea-urethane) s based on AA* and B2B* monomers. J Polym Sci Part A Polym Chem 42:3062–3081
23. Asker M, El-gengaihi SE, Hassan EM, et al (2020) Phytochemical constituents and antibacterial activity of Citrus lemon leaves. Bull Natl Res Cent 44:1–7. https://doi.org/10.1186/s42269-020-00446-1
24. Hagab RH, Kotp YH, Eissa D (2018) Using nanotechnology for enhancing phosphorus fertilizer use efficiency of peanut bean grown in sandy soils. J Adv Pharm Educ Res 8:59–67
25. Decker C, Masson F, Schwalm R (2003) Dual-curing of waterborne urethane-acrylate coatings by UV and thermal processing. Macromol Mater Eng 288:17–28. https://doi.org/10.1002/mame.200290029
26. El Awady ME, Asker MS, Haggag KM, et al (2022) Chemical and Biological Assay for The Degradation of Microwave Synthesized-Hyperbranched Poly (Urethane-Urea) By Local Bacterial Isolates. Egypt J Chem 65:297–305
27. Haggag K, Hashem A, El Shall FN (2017) Thermal stability enhancement of cotton and cotton polyester blend fabrics by hyperbranched poly urethane-urea treatment. Egypt J Chem 60:857–867
28. Feng J, Ye D (2019) Polymerizable ZnO photoinitiators of surface modification with hydroxyl acrylates and photopolymerization with UV-curable waterborne polyurethane acrylates. Eur Polym J 120:109252. https://doi.org/10.1016/j.eurpolymj.2019.109252
29. Amna T, Hassan MS, Sheikh FA, et al (2013) Zinc oxide-doped poly(urethane) spider web nanofibrous scaffold via one-step electrospinning: A novel matrix for tissue engineering. Appl Microbiol Biotechnol 97:1725–1734. https://doi.org/10.1007/s00253-012-4353-0
30. Joudeh N, Linke D (2022) Nanoparticle classification, physicochemical properties, characterization, and applications: a comprehensive review for biologists. J Nanobiotechnology 20:262. https://doi.org/10.1186/s12951-022-01477-8
31. Singh DK, Pandey DK, Yadav RR, Singh D (2012) A study of nanosized zinc oxide and its nanofluid. Pramana - J Phys 78:759–766. https://doi.org/10.1007/s12043-012-0275-8
32. Mashford B, Baldauf J, Nguyen TL, et al (2011) Synthesis of quantum dot doped chalcogenide glasses via sol-gel processing. J Appl Phys 109:94305. https://doi.org/10.1063/1.3579442
33. Goh EG, Xu X, McCormick PG (2014) Effect of particle size on the UV absorbance of zinc oxide nanoparticles. Scr Mater 78–79:49–52. https://doi.org/10.1016/j.scriptamat.2014.01.033
34. Arefi MR, Rezaei-Zarchi S (2012) Synthesis of zinc oxide nanoparticles and their effect on the compressive strength and setting time of self-compacted concrete paste as cementitious composites. Int J Mol Sci 13:4340–4350. https://doi.org/10.3390/ijms13044340
35. Li M, Farooq A, Jiang S, et al (2021) Functionalization of cotton fabric with ZnO nanoparticles and cellulose nanofibrils for ultraviolet protection. Text Res J 91:2303–2314. https://doi.org/10.1177/00405175211001807
36. Tania IS, Ali M, Akter M (2022) Fabrication, characterization, and utilization of ZnO nanoparticles for stain release, bacterial resistance, and UV protection on cotton fabric. J Eng Fiber Fabr 17:15589250221136378. https://doi.org/10.1177/15589250221136378
37. Elshemy NS, Haggage K, El-Sayed H (2022) A Critique on Synthesis and Application of Binders in Textiles Pigment Printing. Egypt J Chem 65:539–549
38. Bao F, Shi W (2010) Synthesis and properties of hyperbranched polyurethane acrylate used for UV curing coatings. Prog Org Coatings 68:334–339. https://doi.org/10.1016/j.porgcoat.2010.03.002
39. Nowak M, Bednarczyk P, Mozelewska K, Czech Z (2022) Synthesis and Characterization of Urethane Acrylate Resin Based on 1,3-Propanediol for Coating Applications. Coatings 12:1860. https://doi.org/10.3390/coatings12121860
40. Bednarczyk P, Wróblewska A, Markowska-Szczupak A, et al (2021) UV curable coatings based on urethane acrylates containing eugenol and evaluation of their antimicrobial activity. Coatings 11:1556. https://doi.org/10.3390/coatings11121556
41. Indhira D, Krishnamoorthy M, Ameen F, et al (2022) Biomimetic facile synthesis of zinc oxide and copper oxide nanoparticles from Elaeagnus indica for enhanced photocatalytic activity. Environ Res 212:113323. https://doi.org/10.1016/j.envres.2022.113323
42. Kafafy H, Shahin AA, Mashaly HM, et al (2021) Treatment of cotton and wool fabrics with different nanoparticles for multifunctional

properties. Egypt J Chem 64:5257–5269. https://doi.org/10.21608/ejchem.2021.72780.3609

43. Verbič A, Gorjanc M, Simončič B (2019) Zinc oxide for functional textile coatings: Recent advances. Coatings 9:550. https://doi.org/10.3390/coatings9090550
44. June YG, Jung KI, Choi M, et al (2020) Effect of urethane crosslinking by blocked isocyanates with Pyrazole-based blocking agents on rheological and mechanical performance of clearcoats. Coatings 10:1–11. https://doi.org/10.3390/coatings10100961
45. Nisansala HMD, Rajapaksha GKM, Dikella DGN V, et al (2021) Zinc Oxide Nanostructures in the Textile Industry. Indian J Sci Technol 14:3370–3395. https://doi.org/10.17485/ijst/v14i46.1052
46. Mudri NH, Abdullah LC, Aung MM, et al (2020) Comparative study of aromatic and cycloaliphatic isocyanate effects on physico-chemical properties of bio-based polyurethane acrylate coatings. Polymers (Basel) 12:1–17. https://doi.org/10.3390/polym12071494
47. Shaikh S, Nazam N, Rizvi SMD, et al (2019) Mechanistic insights into the antimicrobial actions of metallic nanoparticles and their implications for multidrug resistance. Int J Mol Sci 20:2468
48. Yaseen R, Kotp YH, Eissa D (2020) The impact of production of silver nanoparticles using soil fungi and its applications for reducing irrigation water salinity. J Water L Dev 46:216–228. https://doi.org/10.24425/jwld.2020.134216
49. Gold K, Slay B, Knackstedt M, Gaharwar AK (2018) Antimicrobial activity of metal and metal-oxide based nanoparticles. Adv Ther 1:1700033
50. Bukhari A, Ijaz I, Gilani E, et al (2021) Green synthesis of metal and metal oxide nanoparticles using different plants' parts for antimicrobial activity and anticancer activity: A review article. Coatings 11:1374. https://doi.org/10.3390/coatings11111374
51. Mishra PK, Mishra H, Ekielski A, et al (2017) Zinc oxide nanoparticles: a promising nanomaterial for biomedical applications. Drug Discov Today 22:1825–1834
52. Islam F, Shohag S, Uddin MJ, et al (2022) Exploring the Journey of Zinc Oxide Nanoparticles (ZnO-NPs) toward Biomedical Applications. Materials (Basel) 15:2160. https://doi.org/10.3390/ma15062160